Fusion Engineering and Design 86 (2011) 1116–1119

Contents lists available at ScienceDirect

Fusion Engineering and Design

journal homepage: www.elsevier.com/locate/fusengdes

Simserver simulation of a model-based current profile controller in the DIII-D Plasma Control System

Justin Barton[a,*], Yongsheng Ou[a], Chao Xu[a], Eugenio Schuster[a], Michael Walker[b]

[a] Department of Mechanical Engineering and Mechanics, Lehigh University, Bethlehem, PA 18015, USA
[b] General Atomics, San Diego, CA 92121, USA

ARTICLE INFO

Article history:
Available online 25 March 2011

Keywords:
Simserver
Current profile control
Model-based control
Tokamak plasma control

ABSTRACT

Setting up a suitable current profile, characterized by a weakly reversed magnetic shear, has been demonstrated to be a key condition for one possible advanced tokamak operating scenario with improved confinement and possible steady-state operation. Experiments at DIII-D focus on creating the desired current profile during the plasma current ramp-up and early flat-top phases with the aim of maintaining this target profile throughout the subsequent phases of the discharge. The evolution in time of the current profile, or alternatively the safety factor q, is related to the evolution of the poloidal flux, which is modeled in normalized cylindrical coordinates using a partial differential equation referred to as the magnetic flux diffusion equation. A control-oriented model of the current profile evolution in DIII-D was recently developed for the plasma current ramp-up and early flat-top phases and used to synthesize both open-loop and closed-loop control schemes. In this work, we report on the implementation of an advanced model-based current profile controller in the DIII-D Plasma Control System (PCS) and on the assessment of this controller implementation in closed-loop Simserver (simulation server) simulations.

1. Introduction

Active feedback control of the evolution of $q(0)$ and q_{min} during the initial phase of the tokamak discharge has already been tested at DIII-D by changing the plasma conductivity through electron heating [1]. The employed controller requests a power level to the actuator, either electron cyclotron heating (ECH) or neutral beam injection (NBI), that is equal to a preprogrammed feedforward value plus the error in q times a proportional gain. Some present limitations, such as oscillations and instability under certain operating conditions, of this non-model-based, proportional controller motivate the design of a model-based controller that takes into account the dynamics of the whole q profile (not only $q(0)$ and q_{min}) in response to the different actuators and has the potential for improved performance.

Because the actuators used to achieve the desired current profile are constrained by physical limitations, experiments have shown that some of the desired target profiles may not be achievable for all arbitrary initial conditions. Therefore, the objective is to achieve the best possible matching during the early flat-top phase of the total plasma current pulse, which can be treated as a finite-time optimal control problem for a nonlinear partial differential equation (PDE) system. A control-oriented model of the current profile time evolution was developed in [2] and used to design both open-loop and closed-loop control algorithms. Extremum seeking [3] and nonlinear programming [4] techniques have been used to determine open-loop (feedforward) solutions to this optimal control problem. Since these control inputs were computed using the control-oriented model, the actual current profile evolution will not exactly match the desired current profile evolution when the open-loop control inputs are implemented in an experiment. Therefore, a feedback controller is needed to track the desired current profile reference trajectories in the presence of external disturbances. An optimal feedback controller, aimed at rejecting disturbances in the initial poloidal flux profile, was designed in [5]. The total control input is a combination of the optimal feedforward control trajectories plus the feedback correction. In this work we report on the implementation of this advanced model-based controller in the DIII-D Plasma Control System (PCS) and on its effectiveness in closed-loop Simserver (simulation server) simulations. The magnetic diffusion equation is implemented in a Simserver with the ultimate goal of simulating the time evolution of the plasma current profile in response to the active controllers running in the DIII-D PCS.

2. Current profile evolution model

Any quantity that is constant on each magnetic surface can be used to label the flux surfaces. We chose the mean geometric radius, ρ, of the magnetic surfaces as the indexing variable, i.e. $\pi B_{\phi,0}\rho^2 = \Phi$,

* Corresponding author. Tel.: +1 610 758 3707; fax: +1 610 758 6224.
E-mail addresses: justin.barton@lehigh.edu, jeb209@lehigh.edu (J. Barton).

0920-3796/$ – see front matter © 2011 Elsevier B.V. All rights reserved.
doi:10.1016/j.fusengdes.2011.02.091

where Φ is the toroidal magnetic flux and $B_{\phi,0}$ is the reference magnetic field at the geometric plasma center R_0. Let the variable $\hat{\rho}$ denote the normalized radius ($\hat{\rho} = \rho/\rho_b$) where ρ_b is the radius of the last closed magnetic flux surface. The evolution of the poloidal flux in normalized cylindrical coordinates is given by the magnetic diffusion equation [2]

$$\frac{\partial \psi}{\partial t} = \frac{\eta(T_e)}{\mu_0 \rho_b^2 \hat{F}^2} \frac{1}{\hat{\rho}} \frac{\partial}{\partial \hat{\rho}} \left(\hat{\rho} \hat{F} \hat{G} \hat{H} \frac{\partial \psi}{\partial \hat{\rho}} \right) - R_0 \hat{H} \eta(T_e) \frac{\langle \bar{j}_{NI} \cdot \bar{B} \rangle}{B_{\phi,0}} \tag{1}$$

where t is the time, ψ is the poloidal magnetic flux, η is the plasma resistivity, T_e is the electron temperature, μ_0 is the vacuum permeability, $\bar{j}_{NI}$ are the sources of non-inductive current density (NBI, ECH, etc.), $\bar{B}$ is the toroidal magnetic field, and $\langle\rangle$ denotes a flux-surface average. $\hat{F}$, $\hat{G}$, and $\hat{H}$ are geometric factors of the DIII-D tokamak, which are functions of $\hat{\rho}$, and are given in [2]. The boundary conditions are given by

$$\left.\frac{\partial \psi}{\partial \hat{\rho}}\right|_{\hat{\rho}=0} = 0, \quad \left.\frac{\partial \psi}{\partial \hat{\rho}}\right|_{\hat{\rho}=1} = \frac{\mu_0}{2\pi} \frac{R_0}{\hat{G}|_{\hat{\rho}=1} \hat{H}|_{\hat{\rho}=1}} I(t) \tag{2}$$

where $I(t)$ denotes the total plasma current.

The plasma current is mainly driven by induction during the ramp-up and early flat-top phases of the tokamak discharge. Based on experimental observations at DIII-D, simplified scenario-oriented models for the electron temperature, the non-inductive current density, and the plasma resistivity are identified. By employing these simplified models, the magnetic diffusion equation (1) is rewritten as [2]

$$\frac{\partial \psi}{\partial t} = f_1(\hat{\rho}) u_1(t) \frac{1}{\hat{\rho}} \frac{\partial}{\partial \hat{\rho}} \left(\hat{\rho} f_4(\hat{\rho}) \frac{\partial \psi}{\partial \hat{\rho}} \right) - f_2(\hat{\rho}) u_2(t) \tag{3}$$

with boundary conditions

$$\left.\frac{\partial \psi}{\partial \hat{\rho}}\right|_{\hat{\rho}=0} = 0, \quad \left.\frac{\partial \psi}{\partial \hat{\rho}}\right|_{\hat{\rho}=1} = k_3 u_3(t) \tag{4}$$

where

$$\begin{aligned} f_1(\hat{\rho}) &= \frac{k_{eff} Z_{eff}}{k_{T_e}^{3/2} \mu_0 \rho_b^2 \hat{F}^2(\hat{\rho}) \left(T_e^{profile}(\hat{\rho})\right)^{3/2}} \\ f_2(\hat{\rho}) &= \frac{k_{eff} Z_{eff} R_0 k_{NI_{par}} \hat{H}(\hat{\rho}) j_{NI_{par}}^{profile}(\hat{\rho})}{k_{T_e}^{3/2} \left(T_e^{profile}(\hat{\rho})\right)^{3/2}} \\ f_4(\hat{\rho}) &= \hat{F}(\hat{\rho}) \hat{G}(\hat{\rho}) \hat{H}(\hat{\rho}), \quad k_3 = \frac{\mu_0}{2\pi} \frac{R_0}{\hat{G}|_{\hat{\rho}=1} \hat{H}|_{\hat{\rho}=1}} \\ u_1(t) &= \left(\frac{\bar{n}(t)}{I(t)\sqrt{P_{tot}(t)}} \right)^{3/2}, \quad u_2(t) = \frac{\sqrt{P_{tot}(t)}}{I(t)}, \quad u_3(t) = I(t) \end{aligned} \tag{5}$$

and $T_e^{profile}(\hat{\rho})$ and $j_{NI_{par}}^{profile}(\hat{\rho})$ are reference profiles given in [2], $P_{tot}(t)$ is the total power of the non-inductive sources of current (NBI, ECH, etc.), $\bar{n}(t)$ is the line averaged plasma density, $k_{T_e} = 1.7295 \times 10^{10}\ \mathrm{m^{-3} A^{-1} W^{-1/2}}$, $k_{NI_{par}} = 1.2139 \times 10^{18}\ \mathrm{m^{-9/2} A^{-1/2} W^{-5/4}}$, $k_{eff} = 4.2702 \times 10^{-8}\ \Omega\,\mathrm{m\,keV^{3/2}}$, and $Z_{eff} = 1.5$.

The safety factor q is defined as $q(\rho, t) = \partial \Phi / \partial \psi(\rho, t)$ and can be used to specify the toroidal current density. Using the constant relationship between ρ and Φ, $\rho = \sqrt{\Phi/(\pi B_{\phi,0})}$, and the definition of ρ_b, the safety factor is expressed as

$$q(\hat{\rho}, t) = \frac{B_{\phi,0} \rho_b^2 \hat{\rho}}{\partial \psi / \partial \hat{\rho}}. \tag{6}$$

3. Control problem description

The total plasma current evolution can be roughly divided up into two phases: the ramp-up phase and the flat-top phase. The control objectives, as well as the dynamic models describing the time evolution of the current density profile, depend on which phase of the discharge one is operating in. During the ramp-up phase and the first part of the flat-top phase, the control goal is to drive the poloidal magnetic flux profile from an arbitrary initial condition to a predefined target profile in the early flat-top phase. The control objective for the remainder of the flat-top phase is to regulate the current density profile around its desired profile with as little control effort as possible.

In this work, the focus is on the control objectives of the ramp-up and early flat-top phases of the discharge. The control actuators for this phase are $I(t)$, $P_{tot}(t)$, and $\bar{n}(t)$. The waveforms generated by the controller proposed in this work are the references to the respective physical controllers. Since these actuators are physically constrained (see [3] for a description of the actuator constraints), there is no guarantee that the desired target profile can be reached within the prescribed time window. Therefore, an optimal control problem to determine the control laws $I(t)$, $P_{tot}(t)$, and $\bar{n}(t)$ that minimize the cost function

$$J(t_f) = \frac{1}{N} \sum_{i=1}^{N} \left(q(\hat{\rho}_i, t_f) - q^{des}(\hat{\rho}_i) \right)^2 \tag{7}$$

must be solved, where $q^{des}(\hat{\rho}_i)$ is the prescribed target profile. Extremum seeking [3] and nonlinear programming [4] have been used to determine the optimal open-loop control laws $I(t)$, $P_{tot}(t)$, and $\bar{n}(t)$ that minimize (7), and these open-loop control laws have been experimentally tested in the DIII-D tokamak. Fig. 2(a) shows the target final time $q(\hat{\rho}, t_f)$ profile and the experimental final time $q(\hat{\rho}, t_f)$ profile from DIII-D experimental shot 133588 where the optimal open-loop control inputs were employed. The final time t_f was 1.7 s. Since the feedforward control inputs are computed off-line before the experiment is conducted, they cannot be modified during the experiment to account for external disturbances to the system. Therefore, a feedback control algorithm, computed on-line, is needed to track the open-loop current profile reference trajectories and to reject external disturbances to the system.

The controlled variable in the design of the optimal feedback controller is $\theta(\hat{\rho}, t) = \partial \psi / \partial \hat{\rho}$ because of its direct relationship to the safety factor. Substitution of this variable into (3) and subsequent differentiation of the resulting equation with respect to $\hat{\rho}$ leads to a PDE for $\theta(\hat{\rho}, t)$. The PDE describing the dynamics of $\theta(\hat{\rho}, t)$ is reduced to a finite dimensional system via the use of proper orthogonal decomposition (POD) and a Galerkin projection (see, e.g., [4,5] for more details on model reduction). A bilinear system for the tracking error $e(t)$, defined as the difference between the actual $\theta(\hat{\rho}, t)$ and reference $\theta^o(\hat{\rho}, t)$ profiles, is found to enable the design of an optimal feedback controller. The optimal feedback control law is

$$u^*(t) = -R^{-1}(t) B^T(e) s^*(t) e(t) \tag{8}$$

where $R(t)$ is a symmetric positive definite matrix that can be used to satisfy magnitude constraints on the actuators, $B(e)$ is a matrix defined in terms of the reduced order model for $\theta(\hat{\rho}, t)$, and $s^*(t)$ is the solution of a Riccati matrix differential equation. For a detailed derivation of the feedback controller, see [5]. The total control input to the system is the combination of the optimal feedforward control trajectories plus the feedback correction.

4. Simserver

The Simserver architecture is a valuable simulation environment which is used for testing algorithms running in the PCS, and its architecture is shown in Fig. 1. It incorporates a tokamak simulation model that is used to test the PCS in realistic closed-loop simulations. The simulation model accepts control inputs from the PCS and then generates simulated diagnostics. A test switch connects

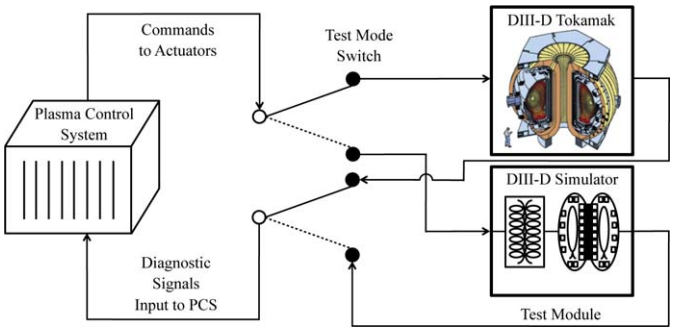

Fig. 1. Simserver architecture.

the PCS (left) to either the DIII-D tokamak (upper right) or the DIII-D simulated tokamak (bottom right) depending on which mode of operation is selected. The Matlab/Simulink modeling environment is used to model the major features of the tokamak, and the only restriction on the Simulink models is that their inputs and outputs must be consistent with the input and output channels in the PCS. This type of simulation is used to determine the effectiveness of controllers and correctness of their real time implementation before experimental tests are conducted [6].

In this work, we seek to use the Simserver to test the implementation in the DIII-D PCS of a control algorithm that combines the optimal feedforward control trajectories [3,4] with the optimal feedback control law (8). In addition, we also aim to determine through simulations the effectiveness with which the nominal trajectories of the system are tracked in the presence of disturbances in the initial conditions. In order to carry out these simulations, a Simulink model of the magnetic diffusion equation (3) is developed and integrated into a Simserver that can interface with the DIII-D PCS. This is done by employing a Simulink *S-function* written in the C programming language.

To construct the model, the governing PDE is discretized in space using a Taylor series expansion while leaving the time domain continuous. The non-dimensional domain of interest, [0,1], is represented as M discrete nodes. The spacing between the nodes, $\Delta\hat{\rho}$, is then defined as $\Delta\hat{\rho} = 1/(M-1)$.

In order to discretize the magnetic diffusion equation in space, Eq. (3) is expanded using the chain rule as

$$\frac{\partial\psi}{\partial t} = f_1 u_1(t)\frac{1}{\hat{\rho}}\left[\hat{\rho}\frac{\partial\psi}{\partial\hat{\rho}}\frac{\partial f_4}{\partial\hat{\rho}} + f_4\frac{\partial\psi}{\partial\hat{\rho}} + \hat{\rho}f_4\frac{\partial^2\psi}{\partial\hat{\rho}^2}\right] - f_2 u_2(t). \tag{9}$$

The space derivative approximations for an arbitrary variable x in the interior node region, $2 \le i \le (M-1)$, are derived as

$$x_{i+1} = x_i + \Delta\hat{\rho}\left.\frac{\partial x}{\partial\hat{\rho}}\right|_i + \frac{(\Delta\hat{\rho})^2}{2}\left.\frac{\partial^2 x}{\partial\hat{\rho}^2}\right|_i + \cdots \tag{10}$$

$$x_{i-1} = x_i - \Delta\hat{\rho}\left.\frac{\partial x}{\partial\hat{\rho}}\right|_i + \frac{(\Delta\hat{\rho})^2}{2}\left.\frac{\partial^2 x}{\partial\hat{\rho}^2}\right|_i + \cdots \tag{11}$$

$$\left.\frac{\partial x}{\partial\hat{\rho}}\right|_i \approx \frac{x_{i+1}-x_{i-1}}{2\Delta\hat{\rho}}, \quad \left.\frac{\partial^2 x}{\partial\hat{\rho}^2}\right|_i \approx \frac{x_{i+1}-2x_i+x_{i-1}}{(\Delta\hat{\rho})^2}. \tag{12}$$

The space derivative approximations for an arbitrary variable x for the boundary node, $i=1$, are derived as

$$x_2 = x_1 + \Delta\hat{\rho}\left.\frac{\partial x}{\partial\hat{\rho}}\right|_1 + \frac{(\Delta\hat{\rho})^2}{2}\left.\frac{\partial^2 x}{\partial\hat{\rho}^2}\right|_1 + \cdots \tag{13}$$

$$x_3 = x_1 + 2\Delta\hat{\rho}\left.\frac{\partial x}{\partial\hat{\rho}}\right|_1 + \frac{(2\Delta\hat{\rho})^2}{2}\left.\frac{\partial^2 x}{\partial\hat{\rho}^2}\right|_1 + \cdots \tag{14}$$

$$\left.\frac{\partial x}{\partial\hat{\rho}}\right|_1 \approx \frac{-3x_1+4x_2-x_3}{2\Delta\hat{\rho}},$$

$$\left.\frac{\partial^2 x}{\partial\hat{\rho}^2}\right|_1 \approx \frac{-3(\partial x/\partial\hat{\rho})|_1 + 4(\partial x/\partial\hat{\rho})|_2 - (\partial x/\partial\hat{\rho})|_3}{2\Delta\hat{\rho}}. \tag{15}$$

Expressions for the spatial derivative approximations for the boundary node, $i=M$, are derived by substituting $-\Delta\hat{\rho}$ for $\Delta\hat{\rho}$ in Eqs. (13) and (14), respectively, to account for the expansions being backward in space instead of forward. The representation of the second derivative with respect to the space coordinate for the boundary nodes (15) is chosen so the boundary conditions (4) of the magnetic diffusion equation can be incorporated into the discretized model. After applying the spatial derivative approximations Eqs. (12) and (15) to (9) and taking into account the boundary conditions (4), we obtain a matrix representation for the finite dimensional model

$$\dot{\alpha}(t) = P\alpha(t)v_1(t) + Nv_2(t) + Zv_3(t). \tag{16}$$

The vector $\alpha = [\psi_1, \ldots, \psi_M]^T \in \mathbb{R}^{M\times 1}$ is the value of $\psi(\hat{\rho}, t)$ at the M discrete nodes, the vector $[v_1(t), v_2(t), v_3(t)]^T = [u_1(t), u_2(t), u_1(t)u_3(t)]^T \in \mathbb{R}^{3\times 1}$ is the control input, and $P \in \mathbb{R}^{M\times M}$, $N \in \mathbb{R}^{M\times 1}$, and $Z \in \mathbb{R}^{M\times 1}$ are the system matrices. This discretization process results in M ordinary differential equations that can be integrated in time to simulate the current profile evolution in response to the control actuator signals.

The Simulink model is required to output the poloidal flux on the magnetic axis and plasma boundary as well as the safety factor q at 32 evenly spaced points on the domain $\psi_{norm} \in [0, 31/32]$ to be fully compatible with the data provided by the real time EFIT reconstruction in the PCS where

$$\psi_{norm} = \frac{\psi - \psi_0}{\psi_{bdry} - \psi_0} \tag{17}$$

and ψ_0 is the poloidal flux on the magnetic axis and ψ_{bdry} is the poloidal flux at the plasma boundary. This is accomplished by using Eqs. (6) and (12) for the interior nodes, Eqs. (6) and (15) for the boundary nodes, and then interpolating the profile onto the desired ψ_{norm} grid.

5. Simulation results

The DIII-D PCS is constructed using the C programming language; therefore, the optimal feedback controller (8) was first implemented in a Simulink C *S-function* to test the control algorithm implementation in the PCS's programming language. Once the algorithm was tested in Simulink, it was inserted into the PCS. Since the control algorithm is a function of the error between the measured value of $\theta(\hat{\rho}, t)$ and the open-loop target value of $\theta(\hat{\rho}, t)$, the Simserver is set up to output $\theta(\hat{\rho}, t)$ (at 32 spatial points for $\hat{\rho} \in [0, 31/32]$) rather than $q(\psi_{norm})$.

The experimental time interval associated with the plasma current ramp-up and early flat-top phases is $[t_i, t_f] = [0.5\,\text{s}, 1.7\,\text{s}]$, and it is the time interval used for this simulation study. The nominal (desired) initial poloidal flux profile, used to compute the optimal open-loop control trajectories [3,4], and the disturbed initial poloidal flux profile, used to test the controller, are shown in Fig. 2(b). A closed-loop Simserver simulation is conducted to determine the performance of the combined feedforward plus feedback controller based on its ability to recover the desired final time $\theta(\hat{\rho}, t_f)$ profile in the presence of this disturbance. Fig. 2(c) shows the final time $\theta(\hat{\rho}, t_f)$ (desired) profile achieved by the open-loop controller for the nominal initial flux profile and the final time $\theta(\hat{\rho}, t_f)$ profile achieved by the closed-loop controller for the

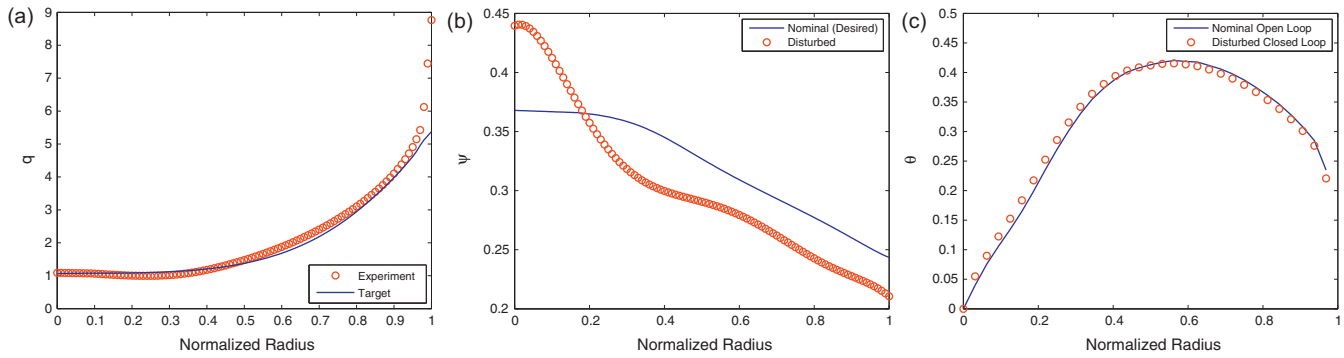

Fig. 2. (a) Experimental final condition $q(\hat{\rho}, t_f)$, (b) simulation initial condition $\psi(\hat{\rho}, t_i)$, and (c) simulation final condition $\theta(\hat{\rho}, t_f)$.

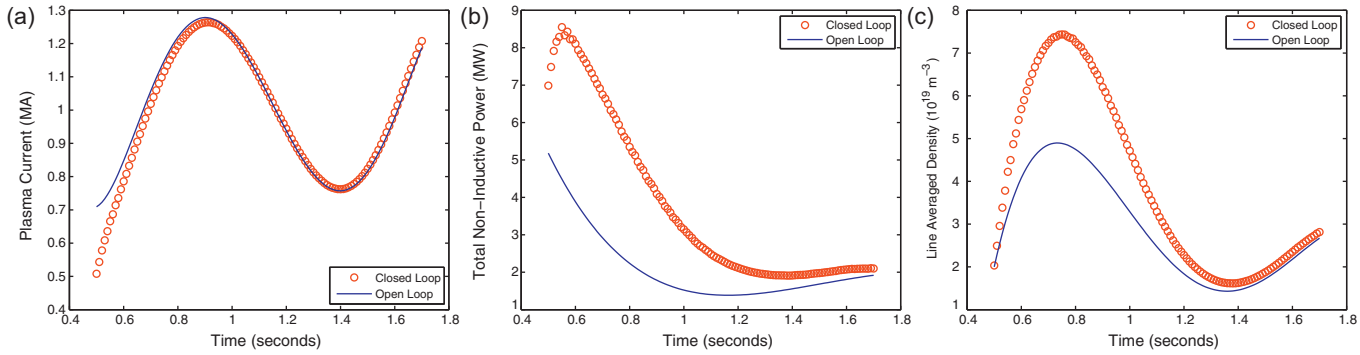

Fig. 3. Control trajectory comparison: (a) plasma current (MA), (b) total non-inductive power (MW), and (c) line averaged density (10^{19} m^{-3}).

disturbed initial flux profile. As can be seen from the figure, the closed-loop controller is able to recover the nominal (desired) final-time profile even in the presence of the disturbance. A comparison of the open-loop and closed-loop control trajectories for $I(t)$, $P_{tot}(t)$, and $\bar{n}(t)$ is shown in Fig. 3. The figure shows that the feedforward control trajectories are modified by the feedback component of the closed-loop controller in the early stages of the simulation to overcome the disturbance in the initial condition as expected. As the simulation progresses, the closed-loop control inputs converge to the open-loop control signals, which indicates that the closed-loop controller is effectively tracking the nominal (desired) current profile evolution after rejecting the initial disturbance.

6. Conclusions and future work

A Matlab/Simulink *S-function* modeling the magnetic diffusion equation is implemented in a Simserver that can interface with the DIII-D PCS. An optimal controller combining both feedforward and feedback actuation is implemented in the DIII-D PCS, and the proposed controller is successfully tested using the Simserver. Our future work will consist of first interfacing the feedback controller with the available real time data $q(\psi_{norm})$ and then experimentally testing the proposed controller in the DIII-D tokamak.

Acknowledgments

Work supported by the NSF CAREER award program (ECCS-0645086) and the US DoE (DE-FG02-09ER55064).

References

[1] J. Ferron, et al., Feedback control of the safety factor profile evolution during formation of an advanced tokamak discharge, Nuclear Fusion 46 (10) (2006) 13–17.
[2] Y. Ou, et al., Towards model-based current profile control at DIII-D, Fusion Engineering and Design 82 (2007) 1153–1160.
[3] Y. Ou, et al., Design and simulation of extremum-seeking open-loop optimal control of current profile in the DIII-D tokamak, Plasma Physics and Controlled Fusion 50 (2008) 115001.
[4] C. Xu, et al., Ramp-up phase current profile control of tokamak plasmas via nonlinear programming, IEEE Transactions on Plasma Science 38 (2010) 163–173.
[5] Y. Ou, et al., Optimal tracking control of current profile in tokamaks, IEEE Transactions on Control Systems Technology 19 (2011) 432–441.
[6] M. Walker, et al., Advances in integrated plasma control on DIII-D, Fusion Engineering and Design 82 (2007) 1051–1057.